Thermodynamic and Structural Properties of Eu^{3+}, Gd^{3+} and Tb^{3+} Complexes with 1,4,7,10-Tetra(2-glutaryl)-1,4,7,10-tetraazacyclododecane in Solution: EXAFS, Luminescence, Potentiometric Studies, and Quantum Calculations

Juliette Moreau,[a] Emmanuel Guillon,[a] Philippe Aplincourt,[b] Jean-Claude Pierrard,[a] Jean Rimbault,*[a] Marc Port,[c] and Michel Aplincourt[a]

Keywords: Lanthanides / Imaging agents / EXAFS spectroscopy / Luminescence / Ab initio calculations

The stability of the various complexes formed by racemic solutions of the title ligand (L) with Gd^{3+}, Eu^{3+} and Tb^{3+} was investigated by potentiometry. The reaction of complexation proceeds through the quick formation of metastable species leading, after a slow reorganisation of the macrocycle, to thermodynamically stable complexes. The mean numbers of water molecules coordinated to the lanthanides were determined by luminescence and EXAFS spectroscopy. This last method, applied to solutions of complexes, allowed us to precisely determine the nature of the atoms that surround the metal atom and the distance between the lanthanide ion and the various ligands. These structural data that are in good agreement with the results found using quantum mechanics allow us to propose a reaction mechanism, from the hydrated lanthanide ion to the final stable complexes through intermediate species. The specific stability of these final complexes arises from the formation of transitory bonds between the metal ion and two pendant arms, which bear carboxylate groups. The stability constants of the final complexes have high values, close to those obtained with DOTA [log $\beta_{110}(EuL^{5-}) = 24.01$; log $\beta_{110}(GdL^{5-}) = 24.03$; log $\beta_{110}(TbL^{5-}) = 23.97$]. This induces a notable in vivo dissociation inertness, which is essential for a potential contrast agent in magnetic resonance imaging.

Introduction

For over two decades, there has been a continuous interest in the study of lanthanide complexes, particularly those of gadolinium(III) with tetraazamacrocyclic ligands, due to their use as paramagnetic contrast agents in diagnostic magnetic resonance imaging (MRI).[1] The main clinically approved gadolinium contrast agents have low molecular weights, and are non-specific agents, which diffuse rapidly in the vascular endothelium.[2] This property limits their use in magnetic resonance coronary angiography and functional imaging.[3] This disadvantage is overcome by the development of Blood Pool Agents, characterised by a high molecular weight, and, consequently, a limited diffusion rate through the endothelium.[4]

The potential contrast agent studied, 1,4,7,10-tetra(2-glutaryl)-1,4,7,10-tetraazacyclododecane, called P730, is a tetracarboxylated derivative of DOTA and a precursor in the synthesis of new MRI macromolecular contrast agents.[3−5] Recent publications, which involved NMR spectroscopy, relaxometry, and luminescence spectrophotometry,[6,7] and which dealt with the structure and dynamics of the numerous stereoisomers formed by this ligand with europium, gadolinium, and terbium, have highlighted the important role of the rate of water exchange.

The ligand P730 may exist as six different stereoisomers, determined by the configuration at each of the stereogenic centres of the carbon atom, (*RRRR*) [(*SSSS*)] and (*RSSS*) [(*SRRR*)] and the achiral diastereoisomers, (*RSRS*) and (*RRSS*) (Scheme 1).

For a given isomer in solution, each chelate formed with the lanthanide usually adopts the same configuration so that four stereoisomers occur, which may interconvert by concerted ring inversions ($\delta\delta\delta\delta \rightarrow \lambda\lambda\lambda\lambda$) or co-operative arm rotation ($\Delta \rightarrow \Lambda$) (Scheme 2).[6,7]

The ratio of diastereoisomers in solution also varies as a function of the lanthanide ion. For the (*RRRR*) isomer, the ratio of the twisted (m) to the regular (M) square-antiprismatic complex was measured by ^{1}H NMR spectroscopy[7] to be4:1 for Eu and 1.5:1 for Tb.

The aqua ions and simple lanthanide salts are toxic for human use. Consequently, lanthanide ions are complexed

[a] GRECI, Université de Reims Champagne-Ardenne,
B. P. 1039, 51687 Reims Cedex 2, France
Fax: (internat.) + 33-3/26913243
E-mail: jean.rimbault@univ-reims.fr
[b] Laboratoire de Chimie Théorique et des Matériaux Hybrides, UPR 5401 CNRS, Ecole Normale Supérieure de Lyon, 69364 Lyon Cedex 07, France
[c] Centre de Recherche Guerbet
Guerbet, B. P. 50400, 95943 Roissy CdG Cedex, France

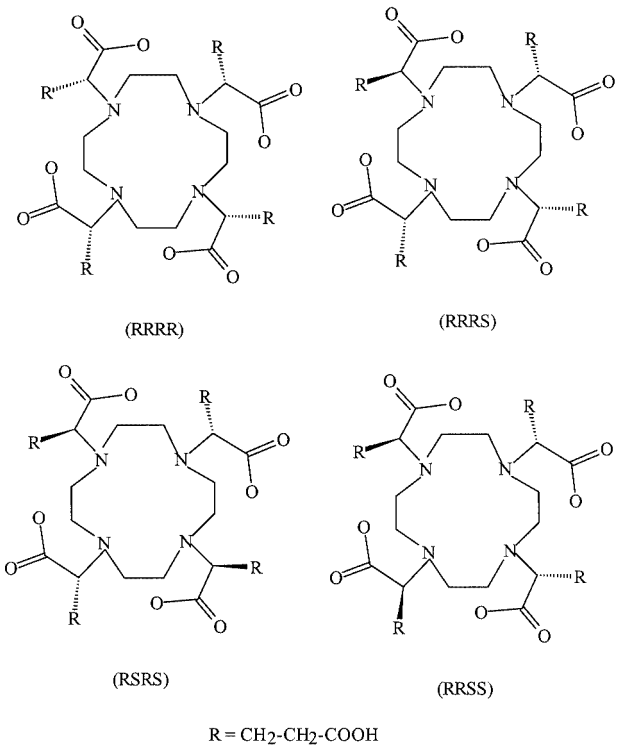

Scheme 1

in order to improve their safety and the toxicity of the lanthanide complexes is related to their stability in vivo. A high thermodynamic stability, slow kinetics, and an inertness to transmetallation, limit the dissociation of these complexes.[8,9]

Some preliminary results on transmetallation and on the stability of Gd-P730 have recently been published.[10] In this paper, we report on the thermodynamic parameters that result from potentiometric measurements performed on the complexes formed after slow complexation reactions (2−3 weeks at 40 °C) between racemic solutions of P730 and the three ions Eu^{3+}, Gd^{3+} and Tb^{3+}. The determination of the logarithms of the protonation constants, a preliminary and indispensable step, leads to the assignment of the log K_h values to the different acidic groups borne by the ligand. The mechanism of complexation of the lanthanide ions proceeds through different stages, leading to the rapid formation of metastable intermediate species, whose formation constants were also calculated.

Results and Discussion

Ligand Protonation Studies in Solution

P730 (LH_8) has 12 potential sites of protonation and, consequently, of complexation: 8 carboxylic groups and 4 tertiary ammonium groups of the macrocycle. The solubility of the neutral ligand is low, close to 10^{-3} mol·L^{-1}. The saturated racemic solution contains 70% of the neutral species LH_8 and also the minor anions LH_7^- (20%) and LH_6^{2-} (10%).

The logarithmic values of the overall protonation constants and of the corresponding successive protonation constants for DOTA and ligand P730, determined in 0.1 mol·L^{-1} Me_4NCl at 25 ± 0.1 °C from the data of 10 titrations, are listed in Table 1. An example of a titration curve is shown in Figure 1.

The protonation sequence of L^{8-} is similar that for the DOTA ligand, which was clearly evidenced by means of NMR spectroscopic studies in solution[11](Table 1). The first two protons are probably bound to two nitrogen atoms of the macrocycle (β_{011}, β_{012}) (see Scheme 1); the next four may correspond to the protonation of the external carboxylate groups [COOH(3): β_{013}, β_{014}, β_{015}, β_{016}]; at pH values < 4, the two central carboxylate groups bound to the tertiary amines are protonated [COOH(2): β_{017}, β_{018}] before the carboxylate group bound to a quaternary ammonium ion in a more acidic medium [COOH(1): β_{019}] (Scheme 3).

In the pH range 3.2−6.5, the titration curve shows a progressive increase similar to that observed with the polycarboxylic acids, which corresponds to the successive and simultaneous neutralisations of the seven carboxylic groups (see Figure 1).

Lanthanide Complexation in Solution

Preliminary tests showed that complexation of the three lanthanides with the ligand proceeds through at least two steps with very different reaction rates.

Formation of Intermediate Species

Figure 1 shows the titration curves obtained 1 h after the mixing of equal volumes of solutions of ligand and metal ion at the same concentrations of approximately 5×10^{-4} mol·L^{-1}. The waiting time between each addition of Me_4NOH is the only variable parameter. The time period is between 0.1 and 30 min. A decrease in pH, accompanying complexation, is observed between the titration curve of the ligand alone and the curves of the solutions that also contain Gd^{3+} at the same concentration.

This set of curves is composed of three parts:

pH range from 3.2 to 5.5, equiv. of OH^- from 0 to 5: The titration curves are well superimposed; the pH values are independent of the waiting time between the additions of base. Protonated metastable complexes are formed during the first and fast kinetic step (less than 30 min). Their notable stability allows the determination of their formation constants.

pH range from 5.5 to 11, equiv. OH^- from 5 to 10: The number and the position of the equivalence points are functions of the waiting time between the additions of base. For short waiting times (0.1−2 min), two equivalence points corresponding to 6 and 8 OH^- equiv. are observed. For longer times, such as 30 min, a single equivalence point remains for 7 OH^- equiv.. This pH range corresponds to the

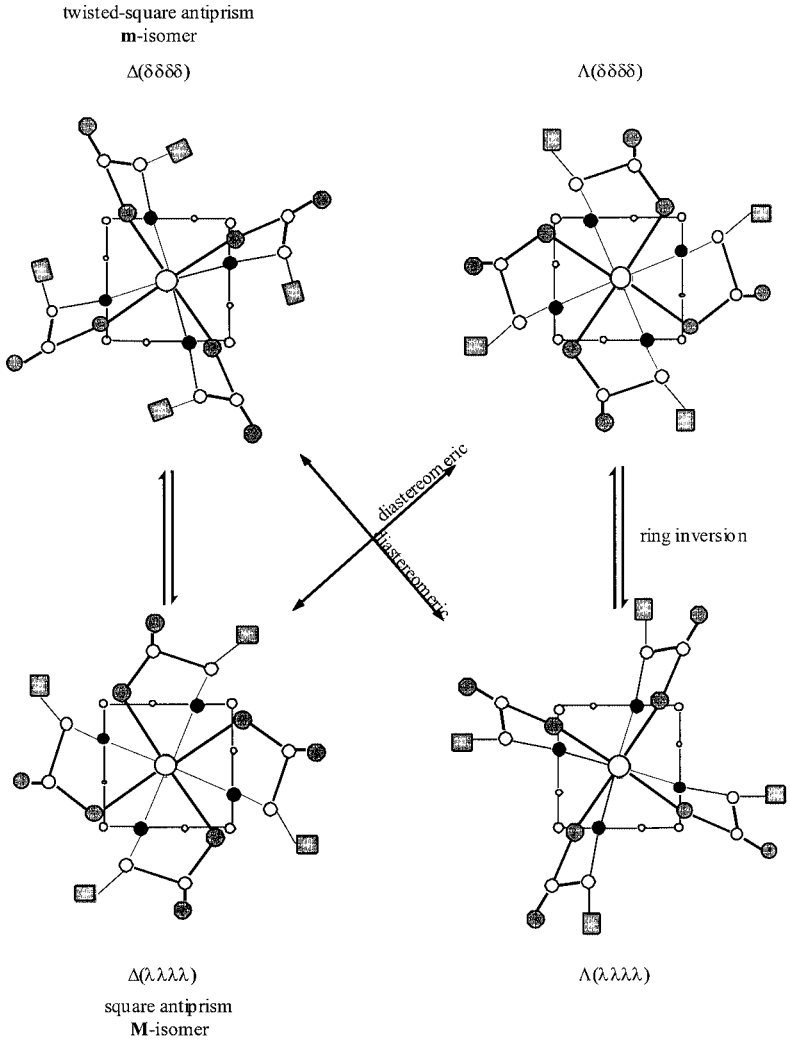

Scheme 2. Shaded squares represent alkyl groups; capped coordinated water molecule has been omitted for clarity

Table 1. Logarithmic values of the overall protonation constants and of the corresponding successive protonation constants for P730 and DOTA (0.1 mol·L^{-1} Me_4NCl; 25 ± 0.1 °C); values in parentheses represent 1 σ standard deviation; $\beta_{01h} = \prod_{1}^{h} K_i$ and log K_h refer to the equilibrium $LH_{h-1} + H^+ \rightleftarrows LH_h$

Logarithms of the overall protonation constants P730	Logarithms of the successive protonation constants P730	Logarithms of the successive protonation constants DOTA[12]	Function
log β_{011} = 12.22(11)	log K_1 = 12.22(11)	log K_1 = 11.45(2)	NH^+
log β_{012} = 21.40(14)	log K_2 = 9.18(4)	log K_2 = 9.64(1)	NH^+
log β_{013} = 27.69(15)	log K_3 = 6.29(3)	−	COOH(3)
log β_{014} = 33.38(15)	log K_4 = 5.69(3)	−	COOH(3)
log β_{015} = 38.42(16)	log K_5 = 5.04(5)	−	COOH(3)
log β_{016} = 43.22(16)	log K_6 = 4.80(5)	−	COOH(3)
log β_{017} = 47.39(16)	log K_7 = 4.17(5)	log K_3 = 4.60(1)	COOH(2)
log β_{018} = 51.32(16)	log K_8 = 3.93(3)	log K_4 = 4.11(1)	COOH(2)
log β_{019} = 54.20(16)	log K_9 = 2.88(2)	log K_5 = 2.29(2)	COOH(1)
−	log K_{10} < 2	log K_6 < 2	COOH(1)

neutralisation of one or two protons bound to nitrogen atoms (the complexation increases the acidity of these protons). These observations indicate the existence of several reaction mechanisms that lead to the formation of unstable species and to significant rearrangements of the macrocyclic ring.

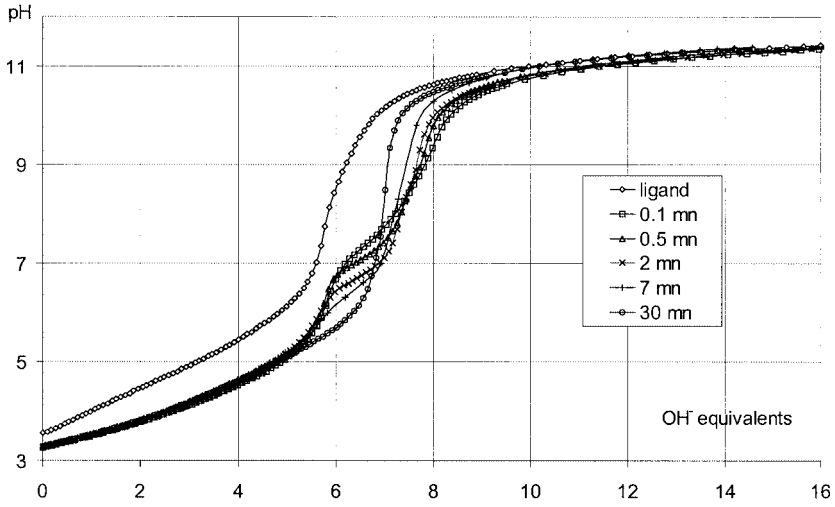

Figure 1. Titration curves of equimolar solutions of P730 and Gd^{3+} (5×10^{-4} mol·L^{-1}) (25 °C, 0.1 mol·L^{-1} Me_4NCl); the upper curve corresponds to the titration of P730 alone; the waiting times values between two successive additions of base vary from 0.1 to 30 min

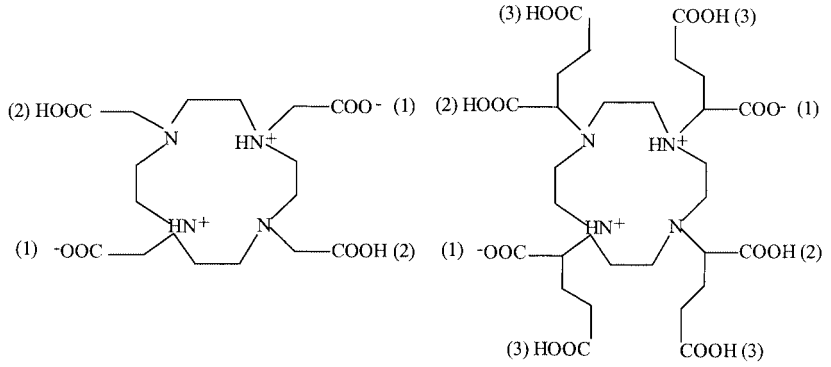

Scheme 3

pH > 11: All the curves are similar to those of the ligand.

A quantitative study is realised from the data of the first part of the titration curves, which corresponds to the formation of metastable complex species (also called intermediate complexes) with a life-time greater than 30 min. The results obtained for the three lanthanides are listed in Table 2.

The logarithms of the overall constants that correspond to the three intermediate Ln^{3+}/P730 systems are very close and follow the general trend Eu > Gd > Tb. The log K_{mh}* values correspond to the protonation of the central ($[MLH_7]^{2+}$*) or external (from $[MLH_6]^{+}$* to $[MLH_3]^{2-}$*) carboxylate groups. These values are indeed lower than those of the ligand. Figure 2 shows the variations of log K

Table 2. Logarithmic values of the overall formation constants β_{mlh}* and of the corresponding successive protonation constants K_{mh}* of the intermediate species MLH_h* (0.1 mol·L^{-1} Me_4NCl; 25 ± 0.1 °C); values in parentheses represent 1 σ standard deviation; log K_{mh}* refers to the equilibrium MLH_{h-1}* + $H^+ \rightleftarrows MLH_h$*

Species	log β_{mlh}*			log K_{mh}*		
	Eu	Gd	Tb	Eu	Gd	Tb
$[MLH_2]^{3-}$*	30.94(2)	30.30(6)	30.25(4)	–	–	–
$[MLH_3]^{2-}$*	36.15(3)	35.77(3)	35.62(4)	5.21(4)	5.46(8)	5.37(6)
$[MLH_4]^{-}$*	40.77(2)	40.36(3)	40.31(2)	4.62(4)	4.60(6)	4.70(5)
$[MLH_5]$*	45.02(3)	44.74(3)	44.59(4)	4.25(4)	4.38(5)	4.27(5)
$[MLH_6]^{+}$*	48.63(2)	48.37(2)	48.31(2)	3.62(4)	3.63(4)	3.72(5)
$[MLH_7]^{2+}$*	51.89(5)	51.70(4)	51.35(10)	3.26(5)	3.34(5)	3.04(11)

versus the number of protonated carboxylates *h* in the case of the ligand P730 alone and of the intermediate gadolinium complexes. The maximum difference is observed at $h = 2$ and 4 ($\Delta\log K = 1.1$ and 1.2, respectively). This indicates notable interactions, maybe the formation of bonds or a network of hydrogen bonds, between two external carboxylate groups and the lanthanide ions.

Formation of Thermodynamically Stable Species

The determination of the stability of the final, stable complexes was done using batch solutions of variable pH.[8,9] Table 3 shows the logarithms of the overall formation constants and of the successive protonation constants.

The values of log β_{mlh} show little variation when the nature of the metal ion changes: the differences observed are of the same order as the calculated standard deviations. The values of log K_{mh} of the external carboxylate groups, from $[MLH]^{4-}$ to $[MLH_4]^{-}$, are only 0.2−0.5 pH units lower than the corresponding ligand log K_h values (see Figure 2). Obviously, these groups are not directly involved in the formation of bonds with the lanthanide ion. The complex $[Gd(P730)]^{5-}$ has a high thermodynamic stability (log $\beta_{110} = 24.03$) as the complex $[Gd(DOTA)]^{-}$ (in Me_4NCl 0.1 mol·L^{-1}, at 25 °C: log $\beta_{110} = 25.58$,[12] 25.30,[13] 24.70,[14] 24.0,[15] 24.67,[9] 25.4,[16] 27.0[17]).

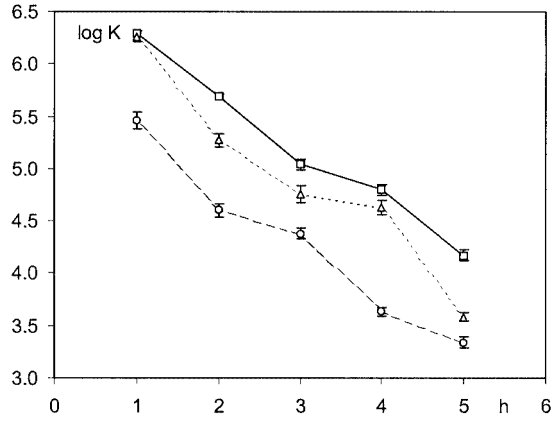

Figure 2. Variation of the logarithms of the successive protonation constants of the carboxylates versus the number of protons *h* in the case of the gadolinium (external carboxylates $h = 1-4$, central carboxylate $h = 5$); squares: ligand P730 (log K_h); circles: intermediate species (log K_{mh}*); triangles: thermodynamically stable species (log K_{mh})

Luminescence Measurements

Horrocks et al.[18,19] have established from experimental results obtained from solid lanthanide complexes that the rate of de-excitation is, to a good approximation, directly proportional to the number of OH oscillators in the first coordination sphere. More recently, an improved approach[20] including other oscillators has shown that, in solution, the intramolecular transfer of energy to the unbound water molecules constitute a significant term in the overall quenching effect. However, this improved approach has also proposed the use of empirical corrections subject to an error of around 25%. A more pragmatic process is to consider that the decay constants determined for Eu^{3+} or Tb^{3+} in D_2O/H_2O mixtures integrate the quenching of water molecules in the first and outer spheres.

The following equation describes the best least-squares lines through the experimental data Δk versus the molar fraction of H_2O in D_2O/H_2O mixtures containing low concentrations of europium or terbium chloride or P730 complexes: $Q = A^*_{Ln}\cdot(k_{H2O} - k_{D2O}) = A^*_{Ln}\cdot\Delta k$. A^*_{Ln} integrates the overall contribution of the vibronic quenching of the OH oscillators, Δk is the slope of the mean straight line, and *q* the hydration number. The values of A^*_{Ln} are calculated by using the hydration numbers determined from EXAFS data[21,22] [8 and 9 for (aquo)terbium and -europium complexes, respectively]. For europium, $A^*_{Eu} = 1.05 \pm 0.02$ ms ($k_{H2O} = 8.77$ ms^{-1}; $k_{D2O} = 0.17$ ms^{-1}) and for terbium, $A^*_{Tb} = 4.86 \pm 0.12$ ms ($k_{H2O} = 2.52$ ms^{-1}; $k_{D2O} = 0.88$ ms^{-1}).

To determine the mean hydration number of the final stable species, racemic solutions of ratio Ln/P730 = 1 were prepared one month before the measurements. The values obtained under these conditions represent a concentration-weighted average of the *q* values of each isomeric species. The results obtained by Woods et al.[7] from solutions of 4 of the 6 pure Eu-P730 stereoisomers correspond to *q* values near to unity in agreement with our average value of *q*(Eu-P730) = 1.04 ± 0.12 ($k_{H2O} = 1.66$ ms^{-1}; $k_{D2O} = 0.67$ ms^{-1}) [Eu-P730 stereoisomers: *q*(*RRRR*) = 1.06; *q*(*RRRS*) = 1.01; *q*(*RRSS*) = 0.92; *q*(*RSRS*) = 1.02]. A notable discrepancy is observed between the corresponding results ob-

Table 3. Logarithmic values of the overall formation constants β_{mlh} and of the corresponding successive protonation constants K_{mh} of the thermodynamically stable species MLH_h (0.1 mol·L^{-1} Me_4NCl; 25 ± 0.1 °C); values in parentheses represent 1 σ standard deviation; log K_{mh} refers to the equilibrium $MLH_{h-1} + H^+ \rightleftarrows MLH_h$

Species	log β_{mlh}			log K_{mh}		
	Eu	Gd	Tb	Eu	Gd	Tb
$[ML]^{5-}$	24.01(5)	24.03(13)	23.97(7)	–	–	–
$[MLH]^{4-}$	29.98(5)	30.28(13)	30.13(6)	5.97(5)	6.26(5)	6.16(6)
$[MLH_2]^{3-}$	35.14(5)	35.55(12)	35.32(6)	5.16(7)	5.27(6)	5.19(7)
$[MLH_3]^{2-}$	40.00(6)	40.31(14)	40.07(7)	4.86(8)	4.76(8)	4.75(9)
$[MLH_4]^{-}$	44.51(3)	44.94(11)	44.62(4)	4.51(6)	4.63(7)	4.54(7)
$[MLH_5]$	47.94(4)	48.52(13)	48.31(5)	3.44(3)	3.58(4)	3.70(4)

tained with the isomers of Tb-P730[7] [Tb-P730 stereoisomers: $q(RRRR) = 0.60$; $q(RRRS) = 0.75$; $q(RRSS) = 1.00$; $q(RSRS) = 0.95$]. Our result obtained from the mixture of the conformers, q(Tb-P730) = 0.96 ± 0.06 (k_{H2O} = 0.46 ms^{-1}; k_{D2O} = 0.27 ms^{-1}), seems to point out that the isomers (*RRRR*) and (*RRRS*) are minor species.

In order to understand the mechanism of formation of the intermediate species formed between europium and the ligand, the mean number of water molecules coordinated to the metal atom was determined under various experimental conditions. The measurements of luminescence were carried out with three series of solutions of ratio P730/Eu^{3+} equal to 10 ([P730] = 10^{-3} mol·L^{-1}), to minimise the concentration of free metal ions at low pH values (Table 4).

Table 4. Experimental and calculated values of q; $q_{calcd.}$ (1): values of q calculated from the first hypothesis; $q_{calcd.}$ (2): values of q calculated from the second hypothesis; percentages of Eu^{3+} for each species (P730/Eu^{3+} = 10; [P730] = 10^{-3} mol·L^{-1}), pH = 3.46: Eu^{3+} 8.1; $[EuLH_7(OH_2)_5]^{2+}$* 0.7; $[EuLH_6(OH_2)_5]^{+}$* 43.1; $[EuLH_5(OH_2)_4]$* 43.9; $[EuLH_4(OH_2)_3]^{-}$* 3.9; $[EuLH_3(OH_2)_3]^{2-}$* 0.4; $[EuLH_2(OH_2)_3]^{3-}$* 0.0. pH = 4.87: Eu^{3+} 0.0; $[EuLH_7(OH_2)_5]^{2+}$* 0.0; $[EuLH_6(OH_2)_5]^{+}$* 0.4; $[EuLH_5(OH_2)_4]$* 10.1; $[EuLH_4(OH_2)_3]^{-}$* 22.8; $[EuLH_3(OH_2)_3]^{2-}$* 56.9; $[EuLH_2(OH_2)_3]^{3-}$* 9.8 (the numbers of molecules of water in the formula correspond to the second hypothesis)

pH	Waiting time	q_{exp}	$q_{calcd.}$ (1)	$q_{calcd.}$ (2)
3.46	none	4.6 ± 0.4	5.32	4.80
3.46	1 h	4.5 ± 0.3	5.32	4.80
4.87	1 h	2.8 ± 0.5	5.00	3.11

The q_{exp} value is a concentration-weighted average of the q values of all the intermediate species and of the (aquo)europium ion bound to 9 molecules of water. Two hypotheses for the intermediate complexes were used to simulate these experimental results. In the first hypothesis, the europium ion is bound only by the 4 central carboxylate groups and 5 water molecules, whatever the pH value and the corresponding deprotonated external carboxylate groups. Second hypothesis: the metal ion is bound by the 4 central carboxylate groups, 1 then 2 external carboxylate groups and 4 then 3 molecules of water according to the pH value. This hypothesis is relevant to the results of the potentiometric study, which points out notable interactions between the external carboxylate group and the lanthanide ion. In this case, the number of water molecules coordinated varied for each one of the protonated species: $[EuLH_7(OH_2)_5]^{2+}$*; $[EuLH_6(OH_2)_5]^{+}$*; $[EuLH_5(OH_2)_4]$*; $[EuLH_4(OH_2)_3]^{-}$*; $[EuLH_3(OH_2)_3]^{2-}$*; $[EuLH_2(OH_2)_3]^{3-}$*. The percentages of Eu^{3+} corresponding to each intermediate complex and to the free ion were calculated, from the concentrations of the reactant using the protonation constants and the stability constants, for each solution that was studied (Table 4).

The calculated values of q corresponding to the possible formation of a bond between the external carboxylate group and the metal ion are in good agreement with the experimental mean results. The similarity of the values of q obtained at pH = 3.46 immediately after preparation of the solutions and after waiting 1 h allows the exclusion of the formation of Eu−N bonds, which correspond to a slow kinetic step.

These results are consistent with the fast formation at a pH near 3.5 of an intermediate complex where the metal atom is bound to the 4 central carboxylate groups of the ligand and to 5 molecules of water. At a pH of around 5, the external carboxylic functions are neutralised which allows the formation of 2 transitory carboxylate bonds and reduces the number of coordinated molecules of water to 3.

EXAFS Measurements

EXAFS experiments were carried out on solutions of the final, stable complex formed with each lanthanide. The environment of the nine-coordinate metal ion was specified and the mean distances corresponding to each type of bond metal atom−coordinated atom determined. An additional experiment enabled the environment of the Gd^{3+} ion in a metastable intermediate complex to be specified.

The number and postulated nature of neighbours, the absorber−neighbour distances, and the Debye−Waller factors resulting from the EXAFS fitting procedure are summarised in Table 5. All four complexes have been fitted considering only single scattering paths.

The k^3-weighted EXAFS spectra and the Fourier transforms of solutions of Ln-P730 final complexes are displayed in Figure 3. Absorptions were collected at k = 12.5 $Å^{-1}$, resulting in a good resolution of peaks in the Fourier transforms. The similarity of the experimental $k\chi(k)$ values and their corresponding Fourier transforms allows us to assume that the local structure of the Ln^{3+} ions is almost the same for the three compounds, the slight differences being attributed to the Ln-P730 distance, which reflects the small ionic radius change from the Eu to the Tb ion. In particular, the amplitudes of the EXAFS oscillations appear almost unchanged. Then, there is the same number of nearest neighbours in the three compounds. In fact, Fourier transforms comprise three main peaks: the first one located at 1.2−2.1 Å (peak 1, Figure 3) corresponds to five oxygen atoms, four from the carboxylic moieties and one from a water molecule, the second one located at 2.1−2.6 Å (peak 2) corresponds to the four nitrogen atoms from the macrocyclic cavity, and the third one located at 2.6−3.4 Å is divided into two components, which correspond to the carbon atoms that belong to the macrocyclic cavity (peak 3′) and to the chains that contain the carboxylic groups (peak 3). Within the frame of the single-scattering approach, we analysed the first three coordination spheres. An additional signal is present at a distance between 3.8 and 5.0 Å for the three complexes. This signal is assigned to the multiple scattering signals on the basis of a previous investigation concerning the compound $[Gd(DOTA)]^{-}$,[22] which is confirmed by the multiple scattering paths obtained by FEFF calculations.[46]

The data available in Table 5 confirms the above qualitative discussion. Within the single-scattering approach, the lanthanide ions are surrounded by the four neighbouring nitrogen atoms of the macrocyclic cavity with an average

Table 5. First coordination shell structural data obtained from *R*-space fits of EXAFS spectra; *N* number of neighbours, *R* absorber−neighbour distance, σ Debye−Waller factor; uncertainties are estimated in coordination numbers to ± 10%, in *R* to ± 0.02 Å, and in σ^2 to ± 0.001 $Å^2$

	Ln−O (COOH)			Ln−O (H_2O)			Ln−N		
	N	*R* [Å]	σ^2 [$Å^2$]N	*R* [Å]	σ^2 [$Å^2$]	N	*R* [Å]	σ^2 [$Å^2$]
$[Eu(P730)]^{5-}$	3.92	2.37	0.002 0.96	2.51	0.007	4.04	2.70	0.005
$[Gd(P730)]^{5-}$	4.32	2.38	0.002 1.22	2.44	0.010	4.12	2.68	0.001
$[Tb(P730)]^{5-}$	3.91	2.36	0.007 1.04	2.50	0.010	4.20	2.65	0.009
$[Gd(P730)H_n]^{(5-n)-}$* intermediate	4.07	2.40	0.009 4.98	2.42	0.010	–	–	–

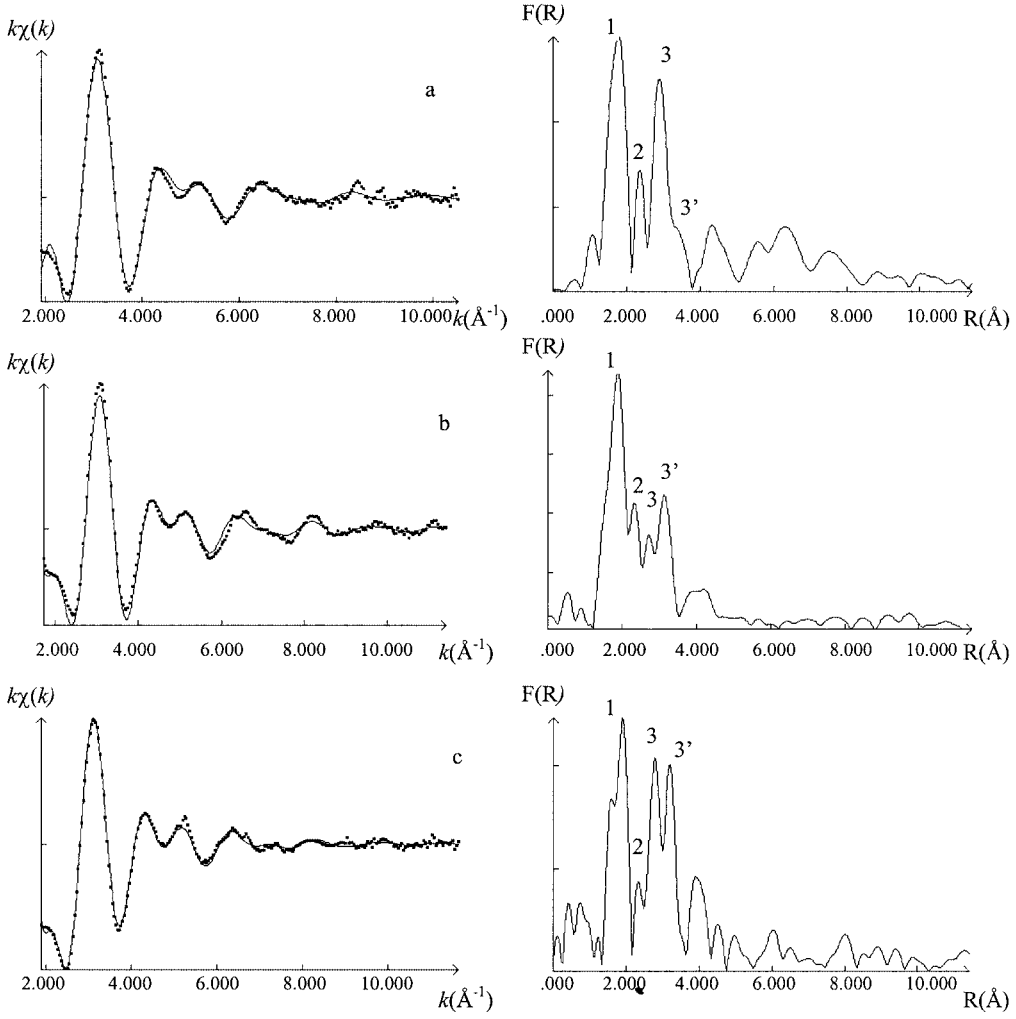

Figure 3. k^3-weighted EXAFS and the corresponding Fourier transforms of solutions containing [P730] = 0.11 mol·L^{-1} and (a) Eu^{3+} = 0.10 mol·L^{-1}, (b) Gd^{3+} = 0.10 mol·L^{-1}, and (c) Tb^{3+} = 0.10 mol·L^{-1} (stable complexes); the Fourier transforms are uncorrected for phase shift; continuous lines represent the models presented in Table 5

Ln−N bond length of 2.68 Å. The decrease of the absorber−coordinated atom distances Ln−N (Eu^{3+} > Gd^{3+} > Tb^{3+}) is in accordance with the slight decrease in ionic radius from the Eu^{3+} to the Tb^{3+} ion.

The absorber ions are also surrounded by four oxygen atoms (carboxylate) with an average Ln−O distance of 2.37 Å. A molecule of water completes the coordination sphere of the three lanthanides. The data are coherent with an EXAFS study of Gd(DOTA) which confirmed that the local environments of the Gd^{3+} centre are similar in solution and in crystals.[7] The Gd−OH_2 distance is in good agreement with the preceding result (2.44 Å), but the bond lengths corresponding to the Eu and Tb complexes are distinctly higher (Eu: 2.51 Å; Tb: 2.50 Å). This could be explained by the fact that water molecules form relatively weak and labile bonds with the lanthanide ions, which gives rise to a

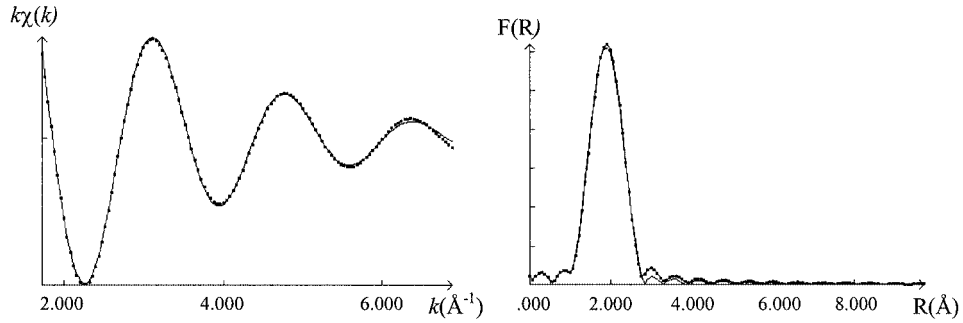

Figure 4. k^3-weighted EXAFS and the corresponding Fourier transform of the first coordination shell of a solution of the intermediate $[Gd(P730)H_n]^{(5-n)-}$* complexes; $[Gd^{3+}] = 9\times10^{-4}$ mol·L^{-1}, [P730] = 9.9×10^{-4} mol·L^{-1}

higher thermal disorder, compared to those of Ln−N or Ln−O (carboxylic), which is in accordance with a fast exchange. Moreover, the two oxygen contributions (carboxylic moieties and water molecules) are difficult to isolate due to their same scattering behaviour. These two phenomena (thermal disorder and scattering behaviour) lead to these relatively unexpected Ln−OH_2 distances.

In accordance with potentiometric studies, an intermediate gadolinium complex has been underlined. Indeed, the radial distribution function of Gd-P730 at 10 °C presents only one main peak located at 1.2−2.6 Å, which corresponds to oxygen atoms from carboxylic groups and water molecules. The k^3-weighted EXAFS, the corresponding Fourier transform, and the fitted curves of the filtered first shell of a solution of the intermediate Gd-P730 species are shown in Figure 4.

The numerical values obtained (Table 5) are in agreement with the main species of a monocapped square-antiprism geometry around the gadolinium centre with four oxygen atoms of carboxylic moieties at 2.40 Å, and five water molecules at 2.42 Å. These results are confirmed by ab initio calculations, which show a relatively stable $[GdLH_6(OH_2)_5]^+$* species with a mean Gd−O(COOH) distance equal to 2.40 Å (see Table 6).

Quantum Chemical Investigation

Quantum calculations were carried out in order to propose a mechanism for the insertion of the lanthanide ion into the ligand. All the complexes optimised by means of ab initio calculations are pictured on Figure 5 (monocapped square-antiprism geometry).The main geometrical parameters computed for these complexes are gathered in Table 6. Ab initio energies computed at the RHF level are reported in Table 7.

In this study, three different complexes {$[GdLH_6(OH_2)_5]^+$*, $[GdLH_4(OH_2)_3]^-$* and $[GdLH_4(OH_2)]^-$} have been found on the potential energy surface (see Figure 5).

The localisation of these complexes allows us to propose a mechanism for the insertion of the gadolinium atom into the ligand. At first, an initial $[GdLH_6(OH_2)_5]^+$* compound is formed in acidic solution. It is a nine-coordinate compound with five water molecules and four central carboxylate oxygen atoms linked to the gadolinium ion. When the pH increases, this complex evolves into the intermediate $[GdLH_4(OH_2)_3]^-$* complex by deprotonation of two external carboxylate groups. These two new carboxylate extremities replace two water molecules for the complexation

Table 6. Main geometrical parameters of experimental (**bold**) and RHF/3-21G (plain) structures of all the complexes optimised in this study; distances are given in Å and angles in °; Φ: twist angle between P_O and P_N planes

Parameter	$[GdLH_6(OH_2)_5]^+$*	$[GdLH_4(OH_2)_3]^-$*	$[GdLH_4(OH_2)]^-$ (*SSSS*)	$[GdLH_4(OH_2)]^-$ (*RRRR*)	**$[GdLH_4(OH_2)]^-$ (*SSSS*)**[a]
Gd−N	4.751	4.396	2.742	2.806	2.67(3)
Gd-*N*-H	4.791	4.349			
Gd−O $_W$up	2.403	2.445	2.400	2.390	2.432
Gd−O $_W$	2.503/2.540	2.508			
Gd−O cent	2.423/2.385	2.506/2.442	2.341	2.325	2.38(2)
Gd−O ext		2.410			
O1−Gd−O2		79.3	85.7	85.7	85.8
O1−Gd−O3			149.3	149.2	144.9
N−C−C−N[b]	−57.3	−61.6	−57.6	−64.2	−59.5(1.4)
Φ			39.8	34.9	38.5
Gd/O plane			0.638	0.635	0.679
Gd/N plane	4.274	3.776	1.705	1.764	

[a] Mean experimental values;[7] standard deviation in parentheses. [b] Torsion angle (for the two intermediate species: N1−C−C−N2)

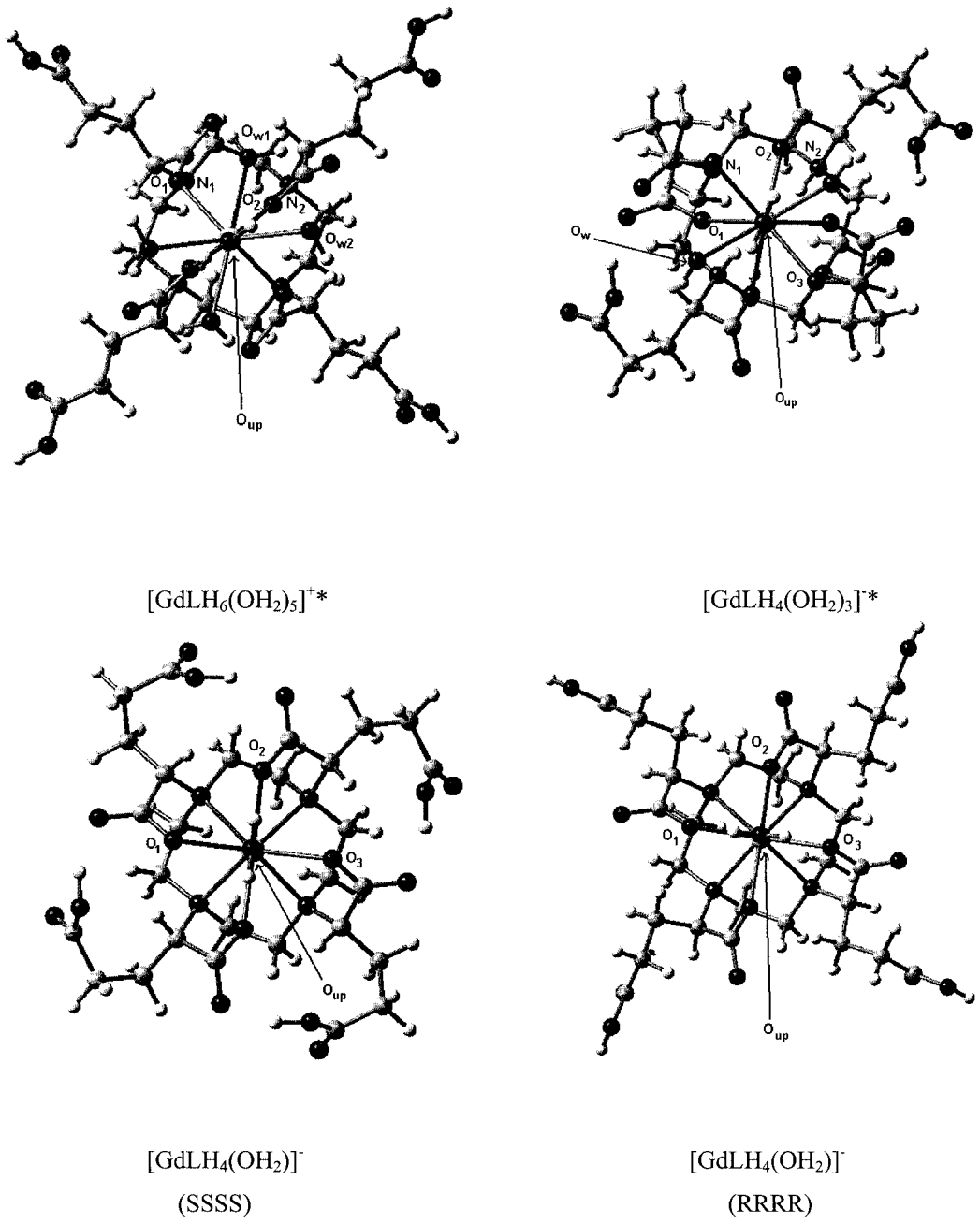

Figure 5. Representation of the three different types of complexes studied theoretically

Table 7. Absolute ab initio energies [Hartree] of all the complexes considered in this study; relative energies between the two (*RRRR*) and (*SSSS*) conformers of the final complex are also reported [kcal/mol]

	$[GdLH_6(OH_2)_5]^{+}$*	$[GdLH_4(OH_2)_3]^{-}$*	$[GdLH_4(OH_2)]^{-}$ (*SSSS*)	$[GdLH_4(OH_2)]^{-}$ (*RRRR*)
RHF/3-21G//RHF/3-21G[a]	−2900.4316609	−2748.18704751	−2597.0289135	−2596.9456351
ΔE			0.0	52.3
RHF/6-31G(d)//RHF/3-21G	−2916.1898152	−2763.0949023	−2611.1539792	−2611.1217399
ΔE			0.0	20.2

[a] See text for a definition of all the acronyms. The X//Y notation means that the energy has been computed at the X level of theory for a structure optimised at the Y level of theory.

of Gd^{3+}. We also tried to optimise another intermediate complex $[GdLH_2(OH_2)]^{-}$* in which the four external carboxylates of the initial complex were deprotonated. However, the existence of such a compound cannot be put forward since we did not succeed in optimising it. Finally, we suggest that the $[GdLH_4(OH_2)_3]^{-}$* complex evolves to a final $[GdLH_4(OH_2)]^{-}$ one by deprotonation of the two nitrogen atoms and reprotonation of the two external carboxylate moieties. The calculation of the distances between the Gd atom and the plane defined by the four nitrogen atoms in these three successive complexes indicates that the gadolinium ion moves more and more into the plane of the ligand as the reaction path proceeds (see Table 6). However, the difference is much less marked from the initial to the intermediate complex (4.274 vs. 3.776 Å) than from the intermediate complex to the final complex (3.776 vs. 1.7−1.8 Å).

For the final $[GdLH_4(OH_2)]^{-}$ complex, two conformers (*RRRR*) and (*SSSS*) in a diastereoisomeric relationship have been optimised in monocapped square-antiprism geometry. Relative energies computed at the RHF/3-21G level show that the (*SSSS*) conformer is more stable than the (*RRRR*) one by 52.3 kcal/mol (see Table 7). It must be pointed out that the energy difference between the two conformers greatly decreases at the RHF/6-31G(d) level (20.2 kcal/mol). This underlines that it is necessary to employ an extended basis set to obtain reliable energies. The main geometrical parameters of the (*SSSS*) species have been reported in Table 6 and compared with an available crystallographic structure recently obtained by Woods et al.[7] Our calculations give Gd−O bonds that are too short and Gd−N bonds that are too long. These results are in line with those found in the case of other gadolinium complexes with similar ligands (DOTA or DOTMA).[23] These two parameters could be corrected by the use of a more extended basis set and the inclusion of the solvent by means of a continuous model[24] but such a calculation would be too time-consuming. Nevertheless, the overall agreement between experimental and theoretical data is good since the average deviation is only 0.05 Å for the distances and 2.2° for the angles. This confirms that the RHF/3-21G method was a good choice to investigate such a compound and allowed us to use this method confidently in order to optimise other complexes. The geometry of the (*RRRR*) has also been reported. The comparison with (*SSSS*) results reveals that the main structural parameters are quite similar in the two conformers. The principal difference comes from the lengthening of the Gd−N bonds in the (*RRRR*) conformer (2.806 vs. 2.742 Å). In the latter, the gadolinium atom is therefore slightly further from the ligand. This is confirmed by the calculation of the distance between this atom and the plane formed by the four nitrogen atoms.

Conclusion

The aim of the magnetic resonance imaging contrast agents is to affect the nuclear magnetic relaxation times of the water protons, increasing the contrast between normal and diseased tissues. Interpreting relaxivity data requires a detailed knowledge of the structures of the complexes in solution. This data does not necessarily correspond to the crystal data because of the lability of these species. The determination of the luminescence decay constants of the lanthanide complexes seems to provide a direct measure of the number of water molecules bound to the metal atom. However, some non-integral values have been interpreted as the result of either a mixture of eight and nine coordinated species, or of a significant contribution of the second-sphere of hydration, or the occurrence of a elongated $Ln-OH_2$ bond. In the present work, the EXAFS data agrees well with the results obtained from the luminescence study ($q \approx 1$); moreover, these results do not show the interaction of the second sphere of hydration and gives reasonable $Ln-OH_2$ bond-length values. An additional EXAFS recording at 10 °C immediately after the preparation of the solution has shown the formation of an intermediate pentahydrate species coordinated to the four central carboxylate groups. The thermodynamic data determined from the potentiometric titrations corresponding to the formation of metastable intermediate complexes indicates strong interactions between two central carboxylate groups and the metal ion. The luminescence measurements confirm the evolution of the number of water molecules coordinated to the lanthanide ion versus time; moreover, they show unambiguously the formation of transitory bonds between the metal ion and one or two external carboxylate groups, which explains the unusual stability of the intermediate complexes. These experimental results as a whole are fully compatible with the complexation mechanism suggested by the quantum chemical investigation.

This whole study allows us to determine the complexation mechanism, in solution, of the lanthanides Gd^{3+}, Eu^{3+}, and Tb^{3+} by the ligand P730. This mechanism is the same for the three lanthanides. Whereas fluorescence experiments were carried out on the europium and terbium complexes, EXAFS was performed on the complexes of the three lanthanides, and the modelling on the gadolinium complexes.

The first step consists of the formation of the species $[LnLH_6(OH_2)_5]^{+}$*, which is presented in Scheme 4.

This complex forms very rapidly, starting at pH = 3.2, in equimolar solutions of Ln^{3+} and P730. In this complex, the four central carboxylic oxygen atoms are bound to the lanthanide atom; the coordination of 9 is ensured by 5 molecules of water. Therefore, the nitrogen atoms, two of which are protonated, do not take part in the complexation. The number of water molecules is characterised by fluorescence and EXAFS experiments, and theoretical calculations predict a stable structure. This complex can be found in solution under the form $[LnLH_6(OH_2)_5]^{+}$* presented above, as well as under the form $[LnLH_7(OH_2)_5]^{2+}$*. The latter species has an additional proton, whose log K_{mh}* is close to 3−3.5. This proton is fixed on an oxygen atom that is not bound to the lanthanide atom, and which belongs to a central carboxylic group. This assumption was put forward by

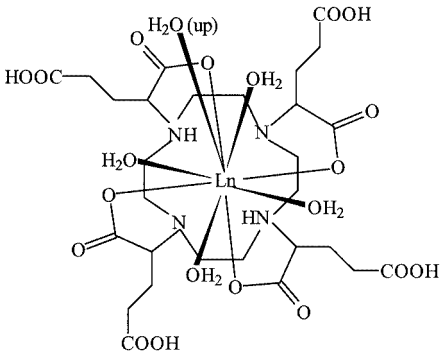

$[GdH_6L(OH_2)_5]^{+}$*

Scheme 4

Szilagyi et al.[27] in the compound Gd(HDOTA). These authors have demonstrated the position of the proton, by fluorescence, UV/Vis spectrophotometry, and NMR spectroscopy. Such a proton can also be found in the structure of the complexes Eu(HP730) in the solid state by Howard et al.[6] and Woods et al.[7]

While the pH increases from 3.2 to 5, the external carboxylic groups are gradually deprotonated. The number of water molecules bound to the lanthanide atom, calculated via fluorescence measurements, goes progressively from 5 to 3. As a result, one, then two additional oxygen atoms of the external carboxylic groups bind to form $[LnLH_5(OH_2)_3]^{2-}$* and then $[LnLH_4(OH_2)_3]^{-}$*, presented in Scheme 5.

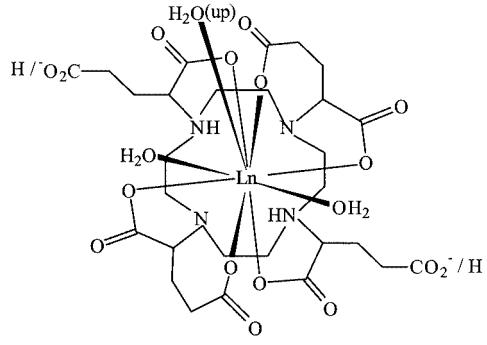

$[GdH_4L(OH_2)_3]^{-}$*

Scheme 5

These species, as well as the ones issued from the deprotonation of the external carboxylic groups $[LnLH_3(OH_2)_3]^{2-}$* and $[LnLH_2(OH_2)_3]^{3-}$*, are put in evidence by potentiometric experiments. The increase of the acidity of two carboxylic groups, shown in Figure 2 (h = 2 and 4), is in accordance with their complexation to the lanthanide. The absence of kinetics noted during these steps shows that there is no modification of the mode of complexation. The nitrogen atoms, two of which are still protonated, are not bound to the lanthanide atom. Our theoretical RHF results confirm the stability of $[GdLH_4(OH_2)_3]^{-}$*.

The coordination of the external carboxylic oxygen atoms was contemplated by Lowe et al.[28,29] in lanthanide complexes with ligands derived from P730, in which a chain $-CH(COO)-CH_2-CH_2-COOH$ linked to the nitrogen atom is replaced with a dansyl substituent.

After several weeks at ambient temperature, or 2 or 3 weeks at 40 °C, all of these compounds evolve towards a series of thermodynamically stable compounds of the formula $[LnLH_n(OH_2)]^{(5-n)-}$ with $0 \leq n \leq 5$. The kinetics corresponds to a significant modification in the nature of the coordinating atoms. The lanthanide atom, which always used to be located above the plane formed by the oxygen atoms of the central carboxylic groups, is now inserted between this plane and the one formed by the nitrogen atoms (Scheme 6).

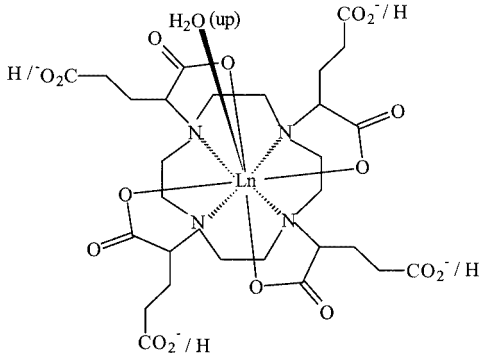

$[GdH_4L(OH_2)]^{-}$

Scheme 6

All these species are identified using potentiometric experiments. In the complex $[LnLH_4(OH_2)]^{-}$ pictured above, the four central carboxylic oxygen atoms and the four deprotonated nitrogen atoms are bound to the lanthanide atom, whereas the coordination number 9 is ensured by one water molecule. The coordinated water molecule is characterised by fluorescence and EXAFS. The latter technique also confirms the nature of the set of atoms linked to the lanthanide atom. Quantum mechanics calculations show the stability of this complex. In the complex $[LnLH_5(OH_2)]$, an additional proton (log K_{mh} close to 3.5) is fixed on the oxygen atom that is not linked to the lanthanide atom, and which belongs to a central carboxylate group.

The variations of the logarithm of the free metal ratio versus pH for the systems Gd/DOTA and Gd/P730 are drawn in Figure 6. Such a plot clearly shows the similarity in the behaviour of the two systems. At physiological pH (7.4), for the same analytical concentrations of metal ion and ligand (5×10^{-4} mol·L^{-1}), the free concentrations of gadolinium(III), in the presence of DOTA and P730, are 3.8×10^{-12} mol·L^{-1} and 3.3×10^{-11} mol·L^{-1}, respectively. These values confirm the high thermodynamic stability of

the ligand studied, providing a potential in vivo dissociation inertness essential for medical applications.

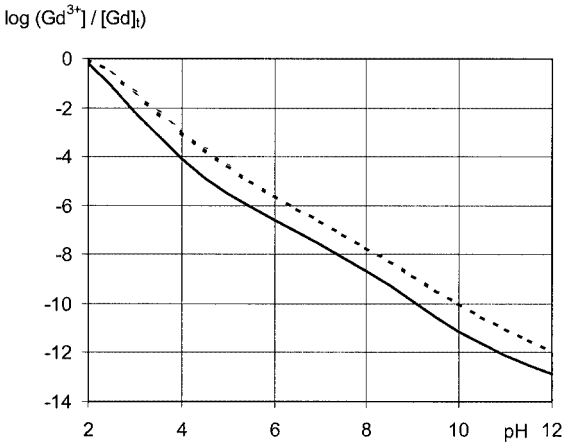

Figure 6. Variation of the logarithm of the free metal ratio versus pH; continuous line: system Gd(DOTA); dashed line: system Gd-P730

Experimental Section

Reagents: All chemicals used were of a pure analytical grade. Distilled and argon-bubbled water was used for the preparation of all solutions. Tetramethylammonium chloride (Fluka Biochemika) was used for ionic strength control in all studies. The standard solutions of the lanthanides (Eu, Gd, Tb) were prepared from trichloride hexahydrate salts (Aldrich). Their concentrations were determined by EDTA titrations using xylenol-orange indicator. Carbonate-free solutions of tetramethylammonium hydroxide (Riedel-de Haën) were used for potentiometric titrations. The ligands DOTA and P730 were a gift of Guerbet SA.

Protometric Measurements: All pH-metric measurements used in the determination of protonation and complexation constants were carried out in a thermo-regulated cell (25 ± 0.1 °C) with an argon stream over the solution to avoid the dissolution of carbon dioxide. The glass microelectrode Metrohm type T has a low alkaline error. The procedures and apparatus used for protometric measurements have been described previously.[30] Titrations of acetic acid with CO_2-free Me_4NOH allowed us to determine the ionic product of water pK_w = 13.78 (1), at 25 ± 0.1 °C in 0.1 mol·L^{-1} Me_4NCl. For each ligand, the protonation constants were determined from several experiments; DOTA: 9 titrations corresponding to 1079 pairs of data, concentration range of the ligand 10^{-3} to 3×10^{-3} mol·L^{-1} in the presence of HCl ($0 <$ [HCl]/[DOTA] < 8). P730:10 titrations corresponding to 1261 pairs of data, concentration range of the ligand 2.2×10^{-4} to 9.7×10^{-4} mol·L^{-1} in the presence of HCl ($0 <$ [HCl]/[P730] < 10.2). The complexation reactions of lanthanides with DOTA and P730 are slow at room temperature. Intermediate species formed in the first hour, after the mixing of the ligand and metal ion, transform into final and stable complexes in some weeks. Titrations performed 1 h after mixing allowed for the determination of the formation constants of the intermediate complexes. At least seven measurements (about 60 points each one) were performed for each system Ln/P730 in the pH range 3.8−6 for complexation experiments. The ligand and metal concentration were about 5×10^{-4} mol·L^{-1}, the ratio ligand/metal being slightly above 1. For each metal, in order to study the final equilibria, three or four batch experiments were performed in which 40 individual solutions, in the approximate pH range 2.8−9, corresponding to single points of conventional titrations, were stored in a thermostat at 40 ± 0.1 °C for 25 d. This time was determined from the pH of reference solutions periodically controlled to ensure the achievement of the conditions of equilibrium.

Protometric Computations: The protometric data were processed by the code Protaf[31] in order to obtain the best-fit chemical model and refined overall stability constants β_{mlh} (β_{mlh} refers to the species $M_mL_lH_h$). The program Protaf,[31] which is based on the weighted least-squares of the residues of the experimental variables (volume of titrant, pH), allows a simultaneous processing of ten titrations, each including 150 pairs of data (volume, pH).

Luminescence Measurements: The measurements were determined in D_2O/H_2O mixtures, the molar fraction of H_2O varying from a value nearing 0 to the value 1, the concentration of the lanthanide chlorides, used as references, or of the corresponding P730 complexes varying from 2×10^{-3} to 2.5×10^{-2} mol·L^{-1} in neutral or basic media. Luminescence spectra for europium and terbium complexes were recorded with a Perkin−Elmer LS50B equipped with a Hamamatsu R928 photo-multiplier and operating in time-resolved mode. Lifetimes were measured at 25 °C by excitation of the sample solution by a short pulse of light (europium species: 394 nm; terbium species: Tb^{3+} 221 nm, Tb-P730 229 nm). The emission was monitored at 616 nm for Eu^{3+} and 544 nm for Tb^{3+} using the program Lemming Ver 1.01. The gate time was 0.1 ms and the slit widths were 15 and 5 nm for Eu^{3+} and less for Tb^{3+}. The rate constants k, inverse of the lifetimes τ, are the average values from 10 series of 20−40 measurements realised for each D_2O/H_2O mixture. The luminescence decay curves were fitted by the following equation using the general curve fitting program Origin: $F = F_o\cdot\exp^{(-kt)}$. High correlation coefficients were determined. The quoted k_{D2O} values were estimated and the k_{H2O} values verified from linear extrapolation of k versus the molar fraction of H_2O.

EXAFS Study: Ln^{3+} L_3-edge spectra were recorded with the XAS4 beamline at the Laboratoire d'Utilisation du Rayonnement Electromagnétique (LURE) of the University of Paris-Sud. Standard operating conditions were a beam energy of 1.85 GeV and a mean intensity of 200−300 mA. The measurements were carried out in the transmission mode with an Si (111) channel-cut monochromator, which was de-tuned to 30% of the maximum intensity for Eu, Gd and 15% for Tb, to remove the higher-order harmonics. The detectors were low-pressure (ca. 0.2 atm) air-filled ionisation chambers. Each spectrum is the sum of three to four recordings in the range from 150 eV below to 600−700 eV above the absorption edge. Spectra were recorded using sampling steps of 2 eV with an integration time of 2.0 s per point. The EXAFS spectra at the Ln^{3+} L_3-edge were measured for the aqueous solution at room temperature at a pH around 9.0. Moreover, the intermediate Gd^{3+} complex spectra was registered at 10 °C and at a pH around 3.2 in order to slow down the kinetic formation of the final complex. The EXAFS data analysis was performed with the "EXAFS pour le Mac" and EXAFS98 programs.[32,33] The $\chi(k)$ functions were extracted from the data[34−36] with a linear pre-edge background, a combination of polynomials (of order 5) and spline atomic-absorption background, and normalised by using the Lengeler−Eisenberger method.[37] The energy threshold, E_0, was taken at the half maximum of the absorption edge. Radial distribution functions $F(R)$ were calculated by Fourier transforms of $k^3w(k)\mu(k)$ in the range 2.0−12.5 Å^{-1}; $w(k)$ is a Kaiser−Bessel apodisation window with a smoothness coefficient $\tau = 2.5$ (k is the photoelectron wave-

number). The peaks corresponding to the successive atomic shells were then isolated and Fourier back-transformed into k space to determine the mean coordination number, N, the bond length, R, and the Debye-Waller factor, σ, by a least-squares fitting procedure using the standard EXAFS formula, without multiple scattering:

$$\chi(k) = S_0^2 \sum_i \left[\frac{N_i}{R_i^2} A_i(k) e^{-2\sigma_i^2 k^2} e^{-2R_i/\lambda(k)} \sin(2kR_i + \Phi_i(k)) \right] \quad (1)$$

The backscattering phase, $\Phi_i(k,R_i)$, and amplitude, $A_i(k,R_i)$, functions have been obtained using two approaches: the experimental and the theoretical one. The experimental back-scattering phase, $\Phi_i(k,R_i)$, and amplitude, $A_i(k,R_i)$, functions have been extracted from the EXAFS data of the model compounds of known crystallographic structure: aqueous rare earth solution,[21] $[Gd(DOTA)]^-$,[22] $[Eu(DOTA)]^-$,[38] and $[Tb(TETA)]^-$.[39] The theoretical back-scattering functions have been calculated using the ab initio code FEFF7,[46] with input data based on the X-ray crystal structure of $[Gd(DOTA)]^-$,[41,42] $[Eu(DOTA)]^-$,[38] and $[Tb(TETA)]^-$.[39]

Computational Methods: Traditional quantum mechanical methods are in general applied with great success for systems containing first-row atoms. However, they cannot be applied for systems with atoms further down the periodic table, e.g. lanthanide atoms, because of the sharp increase in computation time required to treat atoms of large atomic numbers. The effective core potential (ECP) method avoids this problem by replacing the core electrons with an approximate pseudo-potential which is only dependent upon the coordinates of the valence electrons, but takes into account the influence of the core electrons. In this study, geometries of the gadolinium complexes have been optimised in vacuo at the Restricted Hartree−Fock (RHF) level of theory using the (1s−4d, $4f^7$) ECP developed by Dolg et al.[40] with the [5s4p3d]-GTO valence basis set for the metal and the 3-21G basis set for the ligands. Previous studies have shown that inclusion of 4f electrons into the core yields a better description of large molecular systems.[23,44] For energy calculations, the 6-31G(d) basis set has also been used for the ligands. The Restricted Hartree−Fock theory is based on the resolution of the Schrödinger equation. As an exact solution of this equation is not possible, some assumptions are made within this theory. Comparison with experiments indicates that the RHF theory gives reasonably good computed structures and can be confidently used to determine the geometry of large systems. A basis set is the mathematical description of the orbitals within a system used to perform the theoretical calculation. Larger basis sets approximate the orbitals more accurately by imposing fewer restrictions on the location of the electrons in space. The 3-21G and 6-31G(d) are two standard basis sets; the 6-31G(d) one being the most extended one. The methodology described above has previously been used by Cosentino et al.[23−26] in their investigation of 5 complexes of gadolinium with macrocyclic and linear polyamino carboxylate ligands. By comparisons with experimental data, the authors concluded that geometry optimisations can be confidently performed at the RHF/3-21G level because it is a good compromise between accuracy and computational effort. In addition, they showed that RHF/6-31G(d) energy calculations on RHF/3-21G optimised geometries provide a satisfactory representation of the potential energy surface. In addition, other RHF calculations using ECP have been performed on multiply bonded transition metal complexes.[45] Computed structures are in good agreement with corresponding X-ray crystallographic data. All the calculations in this study have been carried out using the Gaussian 98 program.[47]

Acknowledgments

We would like to thank the Groupe Guerbet (Aulnay-sous-Bois, France) for their financial support and the supply of the ligands P730 and DOTA, Dr. Andrew Beeby (University of Durham, Great Britain) for the supply of the Lemming program Ver 1.01. The authors also wish to acknowledge S. Belin (Université Paris Sud, LURE, France) for her help in EXAFS data recording and for helpful discussions.

[1] S. Aime, M. Botta, M. Fasano, E. Terreno, *Chem. Soc. Rev.* **1998**, *27*, 19−29.
[2] H. Gries, *Top. Curr. Chem.* **2002**, *221*, 1−24.
[3] M. Port, C. Corot, O. Rousseaux, I. Raynal, L. Devoldère, J-M. Idée, A. Dencausse, S. Le Greneur, C. Simonot, D. Meyer, *MAGMA* **2001**, *12*, 121−127.
[4] M. Port, D. Meyer, B. Bonnemain, C. Corot, M. Schaefer, O. Rousseaux, C. Simonot, P. Bourrinet, S. Benderbous, A. Dencausse, L. Devoldère, *MAGMA* **1999**, *8*, 172−176.
[5] M. Port, C. Corot, I. Raynal, J.-M. Idée, A. Dencausse, E. Lancelot, D. Meyer, B. Bonnemain, J. Lautrou, *Invest. Radiol.* **2001**, *36*, 445−454.
[6] J. A. Howard, A. M. Kenwright, J. M. Moloney, D. Parker, M. Port, M. Navet, O. Rousseau, M. Woods, *Chem. Commun.* **1998**, 1381−1382.
[7] M. Woods, S. Aimé, M. Botta, J. A. Howard, J. M. Moloney, M. Navet, D. Parker, M. Port, O. Rousseaux, *J. Am. Chem. Soc.* **2000**, *122*, 9781−9792.
[8] A. Bianchi, L. Calabi, L. Ferrini, P. Losi, F. Ugerri, B. Valtancoli, *Inorg. Chim. Acta* **1996**, *249*, 13−15.
[9] A. Bianchi, L. Calabi, C. Giorgi, P. Losi, P. Mariani, P. Paoli, P. Rossi, B. Valtancoli, M. Virtuani, *J. Chem. Soc., Dalton Trans.* **2000**, 697−705.
[10] M. Port, O. Rousseaux, I. Raynal, M. Woods, D. Parker, J. Moreau, J. Rimbault, J-C. Pierrard, M. Aplincourt, *Acad. Radiol.* **2002**, *9 (suppl. 2)*, S300−S303.
[11] J. F. Desreux, E. Merciny, M. F. Loncin, *Inorg. Chem.* **1981**, *20*, 987−991.
[12] J. Moreau, E Guillon, J. C. Pierrard, J. Rimbault, M. Aplincourt, to be published.
[13] K. Kumar, C. A. Chang, L. C. Francesconi, D. D. Dischino, M. F. Malley, J. Z. Gougoutas, M. F. Tweedle, *Inorg. Chem.* **1994**, *33*, 3567−3575.
[14] W. P. Cacheris, S. K. Nickle, A. D. Sherry, *Inorg. Chem.* **1987**, *26*, 958−960.
[15] E. T. Clarke, A. E. Martell, *Inorg. Chim. Acta* **1991**, *190*, 37−46.
[16] M. F. Tweedle, J. J. Hagan, K. Kumar, S. Mantha, C. A. Chang, *Magn. Reson. Imaging* **1991**, *9*, 409−415.
[17] S. Aime, P. L. Anelli, M. Botta, F. Fedelli, M. Grandi, P. Paoli, F. Uggeri, *Inorg. Chem.* **1992**, *31*, 2422−2428.
[18] R. M. Supkowski,W. DeW. Horrocks, *Inorg. Chim. Acta* **2002**, *340*, 44−48.
[19] W. DeW. Horrocks, D. R. Sudnick, *Acc. Chem. Res.* **1981**, *14*, 384−392.
[20] A. Beeby, I. M. Clarkson, R. S. Dickins, S. Faulkner, D. Parker, L. Royle, A. S. de Sousa, J. A. G. Williams, M. Woods, *J. Chem. Soc., Perkin Trans. 2* **1999**, 493−503.
[21] T. Yamaguchi, M. Nomura, H. Wakita, H. Ohtaki, *J. Chem. Phys.* **1988**, *89*, 5153−5159.
[22] S. Bénazeth, J. Purans, M. C. Chalbot, M. K. Nguyen-van-Duong, L. Nicolas, F. Keller, A. Gaudemer, *Inorg. Chem.* **1998**, *37*, 3667−3674.
[23] U. Cosentino, G. Moro, D. Pitea, A. Villa, P. C. Fantucci, A. Maiocchi, F. Uggeri, *J. Phys. Chem. A* **1998**, *102*, 4606−4614.
[24] U. Cosentino, A. Villa, D. Pitea, G. Moro, V. Barone, *J. Phys. Chem. B* **2000**, *104*, 8001−8007.
[25] A. Villa, U. Cosentino, D. Pitea, G. Moro, A. Maiocchi, *J. Phys. Chem. A* **2000**, *104*, 3421−3429.

[26] U. Cosentino, A. Villa, D. Pitea, G. Moro, V. Barone, A. Maiocchi, *J. Am. Chem. Soc.* **2002**, *124*, 4901−4909.
[27] E. Szilagyi, E. Toth, E. Brücher, A. Merbach, *J. Chem. Soc., Dalton Trans.* **1999**, 2481−2486.
[28] M. P. Lowe, D. Parker, *Inorg. Chim. Acta* **2001**, *317*, 163−173.
[29] M. P. Lowe, D. Parker, *Chem. Commun.* **2000**, 707−708.
[30] M. Aplincourt, C. Gérard, R. P. Hugel, J. C. Pierrard, J. Rimbault, A. Bertrandie, B. Magny, P. J. Siret, *Polyhedron* **1987**, *34*, 385−395.
[31] R. Fournaise, C. Petitfaux, *Talanta* **1987**, *34*, 385−395.
[32] A. Michalowicz, in *Logiciels pour la Chimie;* Société Française de Chimie: Paris, **1991**, p. 102.
[33] A. Michalowicz, *J. Chem. Phys. IV* **1997**, *7*, 235.
[34] B. K. Teo, In *Inorganic Chemistry Concepts, EXAFS: Basic Principles and Data Analysis*, Springer-Verlag, Berlin, **1986**, p. 9.
[35] D. C. Königsberger, R. Prins, in *X-ray Absorption* P*rinciples, Applications, Techniques of EXAFS, SEXAFS and XANES*, John Wiley & Sons, New York, **1988**.
[36] Co-Chairmen Report of the International Workshop on Standards and Criteria in X-ray Absorption Spectroscopy: F. W. Lytle, D. E. Sayers, E. A. Stern, *Physica* **1989**, *B158*, 701.
[37] B. Lengeler, P. Eisenberger, *Phys. Rev. B.* **1980**, *21*, 4507−4520.
[38] M. R. Spirlet, J. Rebizant, J. F. Desreux, M. F. Loncin, *Inorg. Chem.* **1984**, *23*, 359−363.
[39] M. R. Spirlet, J. Rebizant, M. F. Loncin, J. F. Desreux, *Inorg. Chem.* **1984**, *23*, 4278−4283.
[40] M. Dolg, H. Stoll, A. Savin, H. Preuss, *Theor. Chim. Acta* **1989**, *75*, 173−194.
[41] J. P. Dubost, J. M. Leger, M. H. Langlois, D. Meyer, *C. R. Acad. Sci. Ser II* **1991**, *312*, 349−354.
[42] C. A. Chang, L. C. Francesconi, M. F. Malley, K. Kumar, J. Z. Gougoutas, M. F. Tweedle, *Inorg. Chem.* **1993**, *32*, 3501−3508.
[43] M. Kaupp, P. V. R. Schleyer, M. Dolg, H. Stoll, *J. Am. Chem. Soc.* **1992**, *114*, 8202−8208.
[44] U. Cosentino, G. Moro, D. Pitea, L. Calabi, A. Maiocchi, *J. Mol. Struc. (THEOCHEM)* **1997**, *392*, 75−85.
[45] T. R. Cundari, M. T. Benson, M. Leigh Lutz, S. O. Sommerer, In Reviews in *Computational Chemistry*, VCH Publisher Inc., New York, **1996**, vol. 8, p. 145−202.
[46] S. I. Zabinsky, J. J. Rehr, A. Ankudinov, R. C. Albers, M. J. Eller, *Phys. Rev. B* **1995**, *52*, 2995−3009.
[47] M. J. Frisch, G. W. Trucks, H. B. Schlegel, G. E. Scuseria, M. A. Robb, J. R. Cheeseman, V. G. Zakrzewski, J. A. Montgomery, R. E. Stratmann, J. C. Burant, S. Dapprich, J. M. Millam, A. D. Daniels, K. N. Kudin, M. C. Strain, O. Farkas, J. Tomasi, V. Barone, M. Cossi, R. Cammi, B. Mennucci, C. Pomelli, C. Adamo, S. Clifford, J. Ochterski, G. A. Petersson, P. Y. Ayala, Q. Cui, K. Morokuma, D. K. Malick, A. D. Rabuck, K. Raghavachari, J. B. Foresman, J. Cioslowski, J. V. Ortiz, B. B. Stefanov, G. Liu, A. Liashenko, P. Piskorz, I. Komaromi, R. Gomperts, R. L. Martin, D. J. Fox, T. Keith, M. A. Al-Laham, C. Y. Peng, A. Nanayakkara, C. Gonzalez, M. Challacombe, P. M. W. Gill, B. G. Johnson, W. Chen, M. W. Wong, J. L. Andres, M. Head-Gordon, E. S. Replogle, J. A. Pople, *Gaussian 98* (Revision A.5), Gaussian Inc., Pittsburgh, PA, **1998**.

Received February 10, 2003

